A new implementation of the secondorder polarization propagator approximation (SOPPA): The excitation spectra of benzene and naphthalene

Martin J. Packer, Erik K. Dalskov, Thomas Enevoldsen, Hans Jo/rgen Aa. Jensen, and Jens Oddershede

Citation: The Journal of Chemical Physics **105**, 5886 (1996); doi: 10.1063/1.472430
View online: http://dx.doi.org/10.1063/1.472430
View Table of Contents: http://scitation.aip.org/content/aip/journal/jcp/105/14?ver=pdfcov
Published by the AIP Publishing

A new implementation of the second-order polarization propagator approximation (SOPPA): The excitation spectra of benzene and naphthalene

Martin J. Packer,[a] Erik K. Dalskov, Thomas Enevoldsen, Hans Jørgen Aa. Jensen, and Jens Oddershede
Department of Chemistry, Odense University, DK-5230 Odense M, Denmark

(Received 4 October 1995; accepted 18 June 1996)

We present a new implementation of the second-order polarization propagator approximation (SOPPA) using a direct linear transformation approach, in which the SOPPA equations are solved iteratively. This approach has two important advantages over its predecessors. First, the direct linear transformation allows for more efficient calculations for large two particle–two hole excitation manifolds. Second, the operation count for SOPPA is lowered by one order, to N^5. As an application of the new implementation, we calculate the excitation energies and oscillator strengths of the lowest singlet and triplet transitions for benzene and naphthalene. The results compare well with experiment and CASPT2 values, calculated with identical basis sets and molecular geometries. This indicates that SOPPA can provide reliable values for excitation energies and response properties for relatively large molecular systems. © *1996 American Institute of Physics.*
[S0021-9606(96)01436-5]

I. INTRODUCTION

The unquestionable success of second-order perturbation theory, MP2, in electronic structure calculations has been demonstrated in many applications in recent years. The computational simplicity of the approach, combined with its well-defined nature, makes it an attractive ''first'' choice for including electron correlation. Both ground state properties, such as dipole moments, and excited state properties, such as the linear response, can be calculated with reasonable accuracy compared with more sophisticated approaches, e.g., like MP4[1] or coupled cluster.[2]

However, the vast majority of MP2 response calculations have been performed on static molecular properties and only recently has this method been extended to allow calculations of dynamic properties;[3–6] in addition, these derivative-based methods cannot give excitation energies or oscillator strengths. The complete active space second-order perturbation theory (CASPT2) approach[7,8] and the second-order polarization propagator approximation (SOPPA),[9,10] on the other hand, can give excitation energies based on the MP2 wave function. It is interesting to note, for instance, that the widespread GAUSSIAN program system[11] has MP2 geometry optimization as a standard tool, but uses the more inferior singly excited CI method for calculation of excited states.

There thus appears to be a need for an easy to use MP2-based method to calculate electronic excitation energies and related properties. We assert that SOPPA[9,10] represents such a method. However, in order to fulfill this goal, it is necessary to have a computationally efficient implementation, parallel in efficiency to that of MP2 energy calculations and geometry optimizations. The current implementations of SOPPA[12,13] need to be updated, in order to incorporate some of the recent advances in computational methodologies. This is the main aim of the present article.

We have expressed the propagator in an unpartitioned form, which allows us to solve the eigenvalue problem by means of a direct linear transformation technique, with trial vectors of length equal to twice the sum of the number of particle–hole $(p-h)$ and two particle–two hole $(2p-2h)$ excitations. The benefit of this approach is that one needs not store the **A**, **B**, and **C** matrices of SOPPA,[9,10] since we directly form the product of the trial vector with these matrices. This gives two main advantages over the previous implementations:

(1) We can handle large $2p-2h$ excitation manifolds more efficiently and thus do calculations of considerably larger molecules than before.
(2) The operation count for the rate determining step is lowered from N^6 to N^5.

Item (1) follows from the fact that the method for constructing the $2p-2h$ corrections to the **A** and **B** matrices in both RPAC[13] and MUNICH[14] (the latter program system being the original implementation of SOPPA[15]), gave either a disk or a time bottleneck for a large basis set or a large number of electrons. The lowering of the operation count is achieved in the construction of the second-order correction to the **B** matrix. This formal simplification may not necessarily lead to a computational saving if the number of iterations needed to solve the eigenvalue problem is larger than the number of occupied molecular orbitals (see Sec. II E). Thus this factor will be more important the larger the molecule becomes.

In addition to these benefits, the new SOPPA implementation has other positive side effects. It represents the first step towards an atomic integral driven SOPPA program, which eliminates the integral transformation and which also makes a parallel implementation of SOPPA feasible. Both

[a]Present address: Department of Chemistry, The University of Sheffield, Sheffield, S3 7HF, U.K.

 0021-9606/96/105(14)/5886/15/$10.00

these steps would lead to even greater computational efficiency.

The present work is aimed at constructing a SOPPA program to calculate excitation energies and frequency-dependent linear response properties. However, the approach that will be outlined in the next section may be extended to frequency-dependent quadratic response properties; that is, for electric response properties, extending from the polarizability, $\alpha(-\omega_\sigma;\omega_1)$, to the first hyperpolarizability, $\beta(-\omega_\sigma;\omega_1,\omega_2)$, where $\omega_\sigma=\Sigma_i\omega_i$. This would require us to use an exponential formalism like the one employed by Olsen and Jørgensen.[16]

In addition to the reformulation of the SOPPA equations in unpartitioned form, we will also present results for the singlet and triplet excitation spectra of benzene and naphthalene. The results compare favourably with experiment for both molecules. Furthermore, we compare our values with results from Roos and co-workers, who have used the CASPT2 approach[17–19] to calculate these properties.

II. THEORY

A. Introduction

The fundamental philosophy of polarization propagator methods is the formulation of methods aimed at direct calculations, i.e., without knowing the individual states and their energies, of excitation properties such as energy differences and frequency dependent second order electric and magnetic properties. The tool is the formulation of equation of motions for average values of operators rather than operators themselves, equations that are formally equivalent to the usual quantum mechanical equation of motions.

The special feature of SOPPA is that we solve the resulting equation of motion for the average value of the observable, typically the dipole moment, through second order in perturbation theory requiring that the response itself, the energy differences and the transition moments are correct through second order.[9,10] This procedure leads to an equation for the response expressed in terms of matrices of the Hamiltonian between states involving $p-h$ and $2p-2h$ excitations out of the Hartree–Fock ground state.

Even though the SOPPA equations have been derived elsewhere[9,10] we shall repeat some of the features of the method here in order to make the presentation consistent and in order to make clear where the differences lie between this and earlier formulations. The previous implementations of SOPPA[12–15] made use of a partitioning technique.[20] The propagator matrix, in the $p-h$ and $2p-2h$ manifolds, is reduced to the same dimension as the one appearing in the first order polarization propagator or random phase approximation (RPA). This is achieved by folding the $2p-2h$ contributions into the $p-h$ space, using the Löwdin[20] partitioning approach. However, if we do not invoke the partitioning technique and thus retain the full propagator matrix it is possible to write the linear response as

$$\langle\langle \mathbf{P};\mathbf{Q}\rangle\rangle_\omega=(\mathbf{P}|\mathbf{h})(\mathbf{h}|\omega\hat{1}-\hat{H}|\mathbf{h})^{-1}(\mathbf{h}|\mathbf{Q}) \tag{1}$$

$$=\sum_{\mu\nu}(-P_\mu^{[1]})(\mathbf{E}^{[2]}-\omega\mathbf{S}^{[2]})^{-1}_{\mu\nu}Q_\nu^{[1]} \tag{2}$$

$$=\sum_{\mu}(-P_\mu^{[1]})N_\mu^Q(\omega). \tag{3}$$

In Eqs. (2) and (3) we have expressed the original superoperator form of SOPPA[9,10] [Eq. (1)] in the notation of Olsen and Jørgensen;[16] this allows us to relate our equations to previous implementations of the direct linear transforms for SCF and MCSCF wave functions.[21,22] The matrix, $\mathbf{E}^{[2]}$, can be written in terms of the excitation and de-excitation operators as follows:

$$E^{[2]}_{\mu\nu}=-\begin{pmatrix} \{q_\mu^\dagger,q_\nu,H\}^{(2)} & \{q_\mu^\dagger,R_\nu,H\}^{(1)} & \{q_\mu^\dagger,q_\nu^\dagger,H\}^{(2)} & \{q_\mu^\dagger,R_\nu^\dagger,H\}^{(1)} \\ \{R_\mu^\dagger,q_\nu,H\}^{(1)} & \{R_\mu^\dagger,R_\nu,H\}^{(0)} & \{R_\mu^\dagger,q_\nu^\dagger,H\}^{(1)} & \{R_\mu^\dagger,R_\nu^\dagger,H\}^{(0)} \\ \{q_\mu,q_\nu,H\}^{(2)} & \{q_\mu,R_\nu,H\}^{(1)} & \{q_\mu,q_\nu^\dagger,H\}^{(2)} & \{q_\mu,R_\nu^\dagger,H\}^{(1)} \\ \{R_\mu,q_\nu,H\}^{(1)} & \{R_\mu,R_\nu,H\}^{(0)} & \{R_\mu,q_\nu^\dagger,H\}^{(1)} & \{R_\mu,R_\nu^\dagger,H\}^{(0)} \end{pmatrix}, \tag{4}$$

where we have used a shorthand notation for the expectation value of a double commutator,

$$\{A,B,C\}=\langle 0|[A,[B,C]]|0\rangle. \tag{5}$$

The overlap matrix, $\mathbf{S}^{[2]}$ is

$$S^{[2]}_{\mu\nu}=\begin{pmatrix} \langle 0|[q_\mu^\dagger,q_\nu]|0\rangle^{(2)} & \langle 0|[q_\mu^\dagger,R_\nu]|0\rangle^{(1)} & \langle 0|[q_\mu^\dagger,q_\nu^\dagger]|0\rangle^{(2)} & \langle 0|[q_\mu^\dagger,R_\nu^\dagger]|0\rangle^{(1)} \\ \langle 0|[R_\mu^\dagger,q_\nu]|0\rangle^{(1)} & \langle 0|[R_\mu^\dagger,R_\nu]|0\rangle^{(0)} & \langle 0|[R_\mu^\dagger,q_\nu^\dagger]|0\rangle^{(1)} & \langle 0|[R_\mu^\dagger,R_\nu^\dagger]|0\rangle^{(0)} \\ \langle 0|[q_\mu,q_\nu]|0\rangle^{(2)} & \langle 0|[q_\mu,R_\nu]|0\rangle^{(1)} & \langle 0|[q_\mu,q_\nu^\dagger]|0\rangle^{(2)} & \langle 0|[q_\mu,R_\nu^\dagger]|0\rangle^{(1)} \\ \langle 0|[R_\mu,q_\nu]|0\rangle^{(1)} & \langle 0|[R_\mu,R_\nu]|0\rangle^{(0)} & \langle 0|[R_\mu,q_\nu^\dagger]|0\rangle^{(1)} & \langle 0|[R_\mu,R_\nu^\dagger]|0\rangle^{(0)} \end{pmatrix} \tag{6}$$

and the transition moment vector, $P_\mu^{[1]}$, is given by

$$P_\mu^{[1]}=\begin{pmatrix} \langle 0|[q_\mu,P]|0\rangle^{(2)} \\ \langle 0|[R_\mu,P]|0\rangle^{(1)} \\ \langle 0|[q_\mu^\dagger,P]|0\rangle^{(2)} \\ \langle 0|[R_\mu^\dagger,P]|0\rangle^{(1)} \end{pmatrix}. \tag{7}$$

The $\{q,q^\dagger\}$ and $\{R,R^\dagger\}$ operators belong to a single $(h-p,p-h)$ and a multiple excitation $(2h-2p,2p-2h$, etc.) manifold, respectively, which will be made more clear in Sec. II B. Thus the subscripts μ,ν are shorthand notations for general excitation indices. The superscripts indicate the order to which each term must be evaluated to fulfill the definition of SOPPA:[9]

(1) The reference wave function, $|0\rangle$, is expanded in a Møller–Plesset perturbation series.
(2) The full propagator (the linear response function) has to be correct through second order in the fluctuation potential.
(3) The transition moment vectors, $P_\mu^{[1]}$, and the propagator matrix, $(\mathbf{E}^{[2]}-\omega\mathbf{S}^{[2]})$, have to be correct through second order in the fluctuation potential for single excitations, but not for higher excitations.

We can thus calculate the response as a dot product between a transition moment vector, $P_\mu^{[1]}$, and a vector, $N_\mu^Q(\omega)$, which is the solution to the set of linear equations

$$N_\mu^Q(\omega)=\sum_\nu\ (\mathbf{E}^{[2]}-\omega\mathbf{S}^{[2]})_{\mu\nu}^{-1}Q_\nu^{[1]}. \tag{8}$$

Similarly, excitation energies are obtained as eigenvalues of the equation

$$(\mathbf{E}^{[2]}-\omega_l\mathbf{S}^{[2]})X_l=0. \tag{9}$$

In order to solve Eqs. (8) and (9), we employ the iterative technique previously used in the MCSCF linear response by Jørgensen and co-workers,[21,22] in which we need to consider the direct linear transformations with the principal propagator, $(\mathbf{E}^{[2]}-\omega\mathbf{S}^{[2]})$. The basic idea is that we introduce an approximation, **b**, to **N** or **X** which is determined through an iterative procedure (for more detail see Sec. II E).

Using the unpartitioned form of the linear response function, we can identify the following block structure of the principal propagator:[9]

$$\mathbf{E}^{[2]}=\begin{pmatrix}\mathbf{A}^{(0,1,2)} & \tilde{\mathbf{C}}^{(1)} & \mathbf{B}^{(1,2)} & \mathbf{0}\\ \mathbf{C}^{(1)} & \mathbf{D}^{(0)} & \mathbf{0} & \mathbf{0}\\ \mathbf{B}^{(1,2)} & \mathbf{0} & \mathbf{A}^{(0,1,2)} & \tilde{\mathbf{C}}^{(1)}\\ \mathbf{0} & \mathbf{0} & \mathbf{C}^{(1)} & \mathbf{D}^{(0)}\end{pmatrix} \tag{10}$$

and

$$\mathbf{S}^{[2]}=\begin{pmatrix}\mathbf{S}^{(0,2)} & \mathbf{0} & \mathbf{0} & \mathbf{0}\\ \mathbf{0} & \mathbf{1} & \mathbf{0} & \mathbf{0}\\ \mathbf{0} & \mathbf{0} & -\mathbf{S}^{(0,2)} & \mathbf{0}\\ \mathbf{0} & \mathbf{0} & \mathbf{0} & -\mathbf{1}\end{pmatrix}. \tag{11}$$

Explicit expressions for the new matrices introduced in Eqs. (10) and (11), in terms of two-electron integrals and orbital energies, are given in Appendix C of Ref. 10. [Please observe that Eq. (C.16) of Ref. 10 has an incorrect sign.] The structure of the transition moment vector, $P_\mu^{[1]}$, allows us to introduce a trial vector for transforming the principal propagator:

$$\mathbf{b}=\begin{pmatrix}b^{ph(0,1,2)}\\ b^{\text{multiple}-ph(1)}\\ b^{hp(0,1,2)}\\ b^{\text{multiple}-hp(1)}\end{pmatrix}. \tag{12}$$

Again, the orders of the terms are explicitly given and the superscript ''multiple'' indicates a higher excitation (i.e., not $p-h$ or $h-p$), which need not be specified at this stage.

In the remainder of this section, we will first consider the definition of SOPPA, and the implications this has for the size of the excitation manifold (Sec. II B). We will then consider the evaluation of the transition moment vectors, $P_\mu^{[1]}$ (Sec. II C). The linear transformation with the principal propagator is derived in two parts: for the $p-h$ parts of the trial vector (Sec. II D 1) and then for the multiple excitation blocks of the trial vector (Sec. II D 2). The first set of transformations includes the random phase approximation,[10] RPA, as well as higher RPA, originally defined by Rose, Shibuya and McKoy.[23,24] The second set includes the linear transformation of the **C** and **D** matrices. The section is concluded with discussion of the iterative algorithm used to solve the eigenvalue problem (Sec. II E) and a comparison of the partitioned and the unpartitioned forms of SOPPA (Sec. II F).

B. Operator manifold and order analysis

The complete excitation manifold consists of single, double, triple, etc., excitations. It is convenient to separate this manifold into the set of single excitations (the particle–hole manifold) and the set of multiple excitations (the two particle–two hole, three particle–three hole, etc., manifold). We can immediately identify the $p-h$ operators,

$$q_\mu^\dagger=q_{ai}^\dagger=E_{ai}^S=a_{a_\alpha}^\dagger a_{i_\alpha}+Sa_{a_\beta}^\dagger a_{i_\beta}, \tag{13}$$

$$q_\mu=q_{ia}=E_{ia}^S, \tag{14}$$

where E^S is the standard singlet $(S=+)$ or triplet $(S=-)$ orbital rotation operator. Throughout this communication the notation will be that $a,b,c,\cdots$ $(i,j,k,\cdots)$ denote orbitals that are unoccupied (occupied) in the Hartree–Fock ground state, while $p,q,r,\cdots$ are used as unspecified orbital indices.

The RPA approach employs only the $p-h$ manifold. This gives the linear response properties of a one-electron perturbation correct through first order in the fluctuation potential.[25] The SOPPA approach aims to extend RPA by evaluating the response through second order. In order to do this, it is necessary to include higher-order corrections to the wave function [Item (1) in Sec. II A] and to extend the excitation manifold. Note, however, that for a two-electron perturbation neither RPA nor SOPPA will be correct through first order. SOPPA will be correct through zeroth order, though, while RPA will not.

The first-order correction to the MP wave function consists of $2p-2h$ terms only. This implies that in the $2p-2h$ and $3p-3h$ blocks of the transition moment vector [Eq. (7)], the first nonzero contribution will be of first order. This will

result from a combination of the excitation operator with the first-order correction to the wave function. For the $4p-4h$ and higher excitations, the transition moment is of at least second order, so that we can immediately neglect these. The transition moment will multiply onto the solution vector, $N_\mu^Q(\omega)$ [Eq. (3)]. The order of $N_\mu^Q(\omega)$ may be derived from inspection of Eq. (8); when the index μ refers to $2p-2h$ or $3p-3h$ operators, either: (i) ν is also a $2p-2h$ index, in which case the transition moment $Q_\nu^{[1]}$ is of at least first order or; (ii) ν is a $p-h$ index, in which case the leading term in the inverse matrix is of first order. Thus the leading term in $N_\mu^Q(\omega)$ must be of first order, giving a response which is of at least second order. This fulfills Item (1) of Sec. II A and implies that we must include the $2p-2h$ and $3p-3h$ manifolds from the multiple excitations.

It has been shown by Nielsen *et al.*,[9] however, that the $2p-2h$ excitations are sufficient to define the SOPPA response. This was demonstrated by orthogonalizing the $3p-3h$ manifold against the $p-h$ excitations (which removes any linear dependencies from the excitation manifold). The lowest nonvanishing term of the transition moment vectors is then of second order.[25] The same will be true for the principal propagator. This means that in the $3p-3h$ trial vectors, there will only be terms of third order and above and so they can be neglected. Reference 9 contains a more thorough discussion of these points. We therefore include only the $2p-2h$ operators from the multiple excitation block. The basic rules we have applied are that: (i) terms involving only $p-h$ operators must be evaluated to second order; (ii) terms involving both $p-h$ and $2p-2h$ operators must be taken to first order only; (iii) and terms involving only $2p-2h$ operators must be of zeroth order.

Orthonormal singlet $2p-2h$ operators can be obtained using the so-called $pp-hh$ coupling, where the two particle operators and the two hole operators are spin coupled independently to obtain the $2p-2h$ spin coupled excitation operators. Using this procedure yields two singlet double excitation operators,[26] $R^\dagger(1)$ which is singlet(pp)–singlet(hh) coupled, and $R^\dagger(2)$ which is triplet(pp)–triplet(hh) coupled. Using the $p-h$ operators given in Eqs. (13) and (14) they may be expressed as

$$R_\mu^\dagger(1)=R_{aibj}^\dagger(1)=\tfrac{1}{2}\{(1+\delta_{ab})(1+\delta_{ij})\}^{-1/2}\times(E_{ai}^+E_{bj}^++E_{aj}^+E_{bi}^+), \tag{15}$$

$$R_\mu^\dagger(2)=R_{aibj}^\dagger(2)=\frac{1}{2\sqrt{3}}(E_{ai}^+E_{bj}^+-E_{aj}^+E_{bi}^+). \tag{16}$$

Similarly, one may show that there are three linearly independent orthonormal triplet $2p-2h$ operators, which can be expressed as[10]

$$T_\mu^\dagger(1)=T_{aibj}^\dagger(1)=\frac{1}{2\sqrt{2}}(1-\delta_{ij})(1-\delta_{ab})\times(E_{aj}^+E_{bi}^-+E_{bi}^+E_{aj}^-), \tag{17}$$

$$T_\mu^\dagger(2)=T_{aibj}^\dagger(2)=\tfrac{1}{2}(1-\delta_{ij})(1+\delta_{ab})^{-1/2}\times(E_{bj}^+E_{ai}^-+E_{aj}^+E_{bi}^-), \tag{18}$$

$$T_\mu^\dagger(3)=T_{aibj}^\dagger(3)=\tfrac{1}{2}(1-\delta_{ab})(1+\delta_{ij})^{-1/2}\times(E_{bj}^+E_{ai}^-+E_{bi}^+E_{aj}^-). \tag{19}$$

C. Transition moment vectors

The transition moment vector, $P_\mu^{[1]}$, is given in Eq. (7). As discussed above, the $p-h$ terms must be evaluated through second order. Two second-order contributions can be identified, one coming from the first-order corrections to the wave function and the other from the second-order corrections. Thus since the commutator $[E_{pq}^S,E_{rs}^s]$ is independent of S, both the singlet (P^+) and triplet (P^-) matrix elements

$$\langle 0^{(1)}|[E_{ia}^S,P^S]|0^{(1)}\rangle=\sum_j P_{aj}^S\rho_{ji}^{(2)}-\sum_b \rho_{ab}^{(2)}P_{bi}^S \tag{20}$$

and

$$\langle HF|[E_{ia}^S,P^S]|0^{(2)}\rangle=\sum_b P_{ab}^S\rho_{bi}^{(2)}-\sum_j \rho_{aj}^{(2)}P_{ji}^S, \tag{21}$$

where $\rho^{(2)}$ is the second-order correction to the one-particle density matrix,

$$\rho_{pq}^{(2)}=\langle 0|E_{pq}^+|0\rangle^{(2)}=\langle 0^{(1)}|E_{pq}^+|0^{(1)}\rangle \tag{22}$$

$$+\langle 0^{(2)}|E_{pq}^+|HF\rangle+\langle HF|E_{pq}^+|0^{(2)}\rangle. \tag{23}$$

The first-order correction to the density matrix is zero, by virtue of the Brillouin condition. Explicit expressions for the correlated one-particle density matrix are given by Jensen *et al.*[27] Note that the occupied-virtual blocks of $\rho^{(2)}$ are equivalent to the Møller–Plesset correlation coefficients, κ_i^a, for the singly excited part of the second-order correction to the wave function.[10]

The $2p-2h$ transition moments must be evaluated to first order, following the discussion of Sec. II B. The expressions will be identical to those given by Oddershede *et al.*[10] If P is a singlet property vector, therefore, the expressions read

$$\langle 0^{(1)}|[R_{aibj}^\dagger(I),P^+]|HF\rangle=N(I)\sum_k (P_{ik}^+\kappa_{kj}^{ab}(I)+P_{jk}^+\kappa_{ik}^{ab}(I))-\sum_c (P_{ca}^+\kappa_{ij}^{cb}(I)+P_{cb}^+\kappa_{ij}^{ac}(I)),\quad I=1,2, \tag{24}$$

where $N(1)=((1+\delta_{ij})(1+\delta_{ab}))^{-1/2}$ and $N(2)=1$. If P is a triplet property vector we get

$$\langle 0^{(1)}|[T^{\dagger}_{aibj}(1),P^{-}]|HF\rangle$$
$$=\frac{\sqrt{2}}{\sqrt{3}}\Bigg[\sum_{k}\ (P^{-}_{ik}\kappa^{ba}_{kj}(2)-P^{-}_{jk}\kappa^{ba}_{ki}(2))$$
$$-\sum_{c}\ (P^{-}_{ca}\kappa^{cb}_{ji}(2)-P^{-}_{cb}\kappa^{ca}_{ji}(2))\Bigg], \tag{25}$$

$$\langle 0^{(1)}|[T^{\dagger}_{aibj}(2),P]|HF\rangle$$
$$=(1+\delta_{ab})^{-1/2}\Bigg[\sum_{k}\ (P_{ik}\kappa^{ba}_{kj}(1)-P_{jk}\kappa^{ba}_{ki}(1))$$
$$+\frac{1}{\sqrt{3}}\sum_{c}\ (P_{ca}\kappa^{cb}_{ji}(2)+P_{cb}\kappa^{ca}_{ji}(2))\Bigg] \tag{26}$$

and

$$\langle 0^{(1)}|[T^{\dagger}_{aibj}(3),P]|HF\rangle$$
$$=(1+\delta_{ij})^{-1/2}\Bigg[-\frac{1}{\sqrt{3}}\sum_{k}\ (P_{ik}\kappa^{ba}_{kj}(2)+P_{jk}\kappa^{ba}_{ki}(2))$$
$$-\sum_{c}\ (P_{ca}\kappa^{cb}_{ji}(1)-P_{cb}\kappa^{ca}_{ji}(1))\Bigg]. \tag{27}$$

In the above expressions, the $\kappa^{ab}_{ij}(I)$, $I=1,2$ elements are the MP2 correlation coefficients, for the first-order correction to the wave function, given by[10]

$$\kappa^{ab}_{ij}(I)=(2I-1)^{1/2}\,\frac{g_{aibj}-(-1)^{I}g_{ajbi}}{\epsilon_i+\epsilon_j-\epsilon_a-\epsilon_b}, \tag{28}$$

where $g_{pqrs}=(pq|rs)$ is a two-electron integral in the Mulliken notation and ϵ_i an SCF orbital energy.

D. Direct linear transformation with $E^{[2]}$ and $S^{[2]}$

The direct linear transformation with $\mathbf{E}^{[2]}$ on the trial vector $\mathbf{b}$ [see the discussion preceding Eqs. (10) and (11)] can be shown to give

$$[\mathbf{E}^{[2]}\mathbf{b}]_{\mu}=\sum_{\nu}\begin{pmatrix} A_{\mu\nu}b^{ph}_{\nu}+B_{\mu\nu}b^{hp}_{\nu}\\ C_{\mu\nu}b^{ph}_{\nu}\\ A_{\mu\nu}b^{hp}_{\nu}+B_{\mu\nu}b^{ph}_{\nu}\\ C_{\mu\nu}b^{hp}_{\nu}\end{pmatrix}+\begin{pmatrix} \widetilde{C}_{\mu\nu}b^{2p2h}_{\nu}\\ D_{\mu\nu}b^{2p2h}_{\nu}\\ \widetilde{C}_{\mu\nu}b^{2h2p}_{\nu}\\ D_{\mu\nu}b^{2h2p}_{\nu}\end{pmatrix}$$
$$=-\begin{pmatrix} \langle 0|[q_{\mu},H^{S}(b)]|0\rangle\\ \langle \mu^{S}|H^{S}(b)|0\rangle\\ \langle 0|[q^{\dagger}_{\mu},H^{S}(b)]|0\rangle\\ -\langle 0|H^{S}(b)|\mu^{S}\rangle\end{pmatrix}$$
$$-\begin{pmatrix} \langle 0|[q_{\mu},H]|0^{R}\rangle\\ \langle \mu^{S}|H|0^{R}\rangle\\ \langle 0^{L}|[q^{\dagger}_{\mu},H]|0\rangle\\ -\langle 0^{L}|H|\mu^{S}\rangle\end{pmatrix}. \tag{29}$$

The $H^{S}(b)$ term is the one-index transformed Hamiltonian[16,21,22]

$$H^{S}(b)=\Bigg[\sum_{ia}\ b_{ai}E^{S}_{ai}+b_{ia}E^{S}_{ia},H\Bigg]$$
$$=\Bigg[\sum_{pq}\ b_{pq}E^{S}_{pq},H\Bigg]=\sum_{pq}\ h_{\widetilde{pq}}E^{S}_{pq}$$
$$+\frac{1}{2}\sum_{pqrs}\ (g_{\widetilde{pq}rs}e^{S,+}_{pqrs}+g_{pq\widetilde{rs}}e^{+,S}_{pqrs}), \tag{30}$$

where

$$e^{S_1,S_2}_{pqrs}=E^{S_1}_{pq}E^{S_2}_{rs}-\delta_{qr}E^{S_1\cdot S_2}_{ps} \tag{31}$$

and the one-index transformed one- and two-electron integrals are given by

$$h_{\widetilde{pq}}=\sum_{o}\ (b_{po}h_{oq}-b_{oq}h_{po}) \tag{32}$$

and

$$g_{\widetilde{pq}rs}=\sum_{o}\ (b_{po}g_{oqrs}-b_{oq}g_{pors}), \tag{33}$$

$$g_{pq\widetilde{rs}}=\sum_{o}\ (b_{ro}g_{pqos}-b_{os}g_{pqro}). \tag{34}$$

The trial vectors **b** comprise both the excitation and deexcitation blocks. We then have the conditions that,

$$b_{ai}=b^{ph}_{ai},$$
$$b_{ia}=b^{hp}_{ia},$$
$$b_{ij}=b_{ab}=0. \tag{35}$$

There are $2p-2h$ contributions in both terms of Eq. (29), since $|0^{R}\rangle$ and $\langle 0^{L}|$ are defined as

$$|0^{R}\rangle=-\sum_{I=1,2}\sum_{\substack{a\geqslant b\\ i\geqslant j}}b^{2p2h}_{aibj}(I)R^{\dagger}_{aibj}(I)|HF\rangle,$$
$$\langle 0^{L}|=\sum_{I=1,2}\sum_{\substack{a\geqslant b\\ i\geqslant j}}b^{2p2h}_{iajb}(I)\langle HF|R_{iajb}(I), \tag{36}$$

in the singlet case and

$$|0^{R}\rangle=-\sum_{I=1,3}\sum_{\substack{a\geqslant b\\ i\geqslant j}}b^{2p2h}_{aibj}(I)T^{\dagger}_{aibj}(I)|HF\rangle,$$
$$\langle 0^{L}|=\sum_{I=1,3}\sum_{\substack{a\geqslant b\\ i\geqslant j}}b^{2p2h}_{iajb}(I)\langle HF|T_{iajb}(I) \tag{37}$$

in the triplet case. Since we are using a spin coupled formalism it is also necessary to have the $2p-2h$ trial vectors divided up according to the extra spin quantum number introduced in Eqs. (15)–(19), that is, the index I in Eqs. (36) and (37). This also means that the doubly excited state $|\mu^{S}\rangle$ is a vector defined as

$$\begin{pmatrix} |\mu^{+}(1)\rangle\\ |\mu^{+}(2)\rangle\end{pmatrix}=\begin{pmatrix} R^{\dagger}_{\mu}(1)|HF\rangle\\ R^{\dagger}_{\mu}(2)|HF\rangle\end{pmatrix} \tag{38}$$

for singlet and

$$\begin{pmatrix} |\mu^-(1)\rangle \\ |\mu^-(2)\rangle \\ |\mu^-(3)\rangle \end{pmatrix} = \begin{pmatrix} T_\mu^\dagger(1)|HF\rangle \\ T_\mu^\dagger(2)|HF\rangle \\ T_\mu^\dagger(3)|HF\rangle \end{pmatrix} \tag{39}$$

for triplet properties. In order to compare directly to higher RPA (HRPA), we separate the linear transformation into two parts. We first consider the contributions coming from the $p-h$ block of the trial vector and then the contributions from the $2p-2h$ block.

1. Contributions from the p−h trial vector

In the second part of Eq. (29), the terms containing a q or $q^\dagger$ operator can be compared directly to the expressions obtained in HRPA, which arise when we consider the propagator to second order in the fluctuation potential, but include only the $p-h$ operators. We therefore only need to consider the transformation of the $p-h$ block of the trial vector with $\mathbf{E}^{[2]}$,

$$[\mathbf{E}^{[2]}\mathbf{b}^{ph}]_{ai} = -\begin{pmatrix} \langle 0|[q_{ia}, H^S(b)]|0\rangle \\ \langle 0|[q_{ai}^\dagger, H^S(b)]|0\rangle \end{pmatrix}. \tag{40}$$

The RPA equations are obtained by evaluating Eq. (40) through first order, which gives

$$-\begin{pmatrix} \langle 0|[q_{ia}, H^S(b)]|0\rangle \\ \langle 0|[q_{ai}^\dagger, H^S(b)]|0\rangle \end{pmatrix} = -2\begin{pmatrix} u_{ai}^S(b) \\ -u_{ia}^S(b) \end{pmatrix}, \tag{41}$$

where $u^S(b^{ph})$ is defined in the form of a Fock matrix[16]

$$u^S(b)_{pq} = h_{\widetilde{pq}} + \sum_j \{2g_{\widetilde{pq}jj} + (1+S1)g_{pq\widetilde{jj}} - g_{\widetilde{pj}jq} - g_{pj\widetilde{jq}}\}. \tag{42}$$

The remaining second-order terms, which define HRPA, are obtained by introducing the first order correction $|0^{(1)}\rangle$,

$$-\begin{pmatrix} \langle HF|[q_{ia}, H^S(b)]|0^{(1)}\rangle \\ \langle 0^{(1)}|[q_{ai}^\dagger, H^S(b)]|HF\rangle \end{pmatrix} = -2\begin{pmatrix} u_{ai}^S(b)^{(2)} \\ -u_{ia}^S(b)^{(2)} \end{pmatrix} \tag{43}$$

with

$$u_{ai}^+(b)^{(2)} = \sum_{dkc} (g_{\widetilde{a}\widetilde{d}kc} + g_{ad\widetilde{kc}})\kappa_{ik}^{dc} - \sum_{lkc} (g_{\widetilde{l}\widetilde{i}kc} + g_{li\widetilde{kc}})\kappa_{lk}^{ac} \tag{44}$$

and

$$u_{ia}^+(b)^{(2)} = \sum_{dkc} (g_{\widetilde{d}\widetilde{a}ck} + g_{da\widetilde{ck}})\kappa_{ik}^{dc} - \sum_{lkc} (g_{\widetilde{l}\widetilde{i}ck} + g_{il\widetilde{ck}})\kappa_{ik}^{ac}. \tag{45}$$

The triplet matrix elements are given by

$$u_{ai}^-(b)^{(2)} = \sum_{dkc} (g_{ad\widetilde{kc}}\ {}^t\kappa_{ki}^{cd} - g_{\widetilde{a}\widetilde{d}kc}\kappa_{ki}^{cd}) - \sum_{lkc} (g_{\widetilde{l}\widetilde{i}kc}\kappa_{kl}^{ca} - g_{li\widetilde{kc}}\ {}^t\kappa_{kl}^{ca}) \tag{46}$$

and

$$u_{ia}^-(b)^{(2)} = \sum_{dkc} (g_{da\widetilde{ck}}\ {}^t\kappa_{ik}^{dc} - g_{\widetilde{d}\widetilde{a}ck}\kappa_{ik}^{dc}) - \sum_{lkc} (g_{\widetilde{l}\widetilde{i}ck}\kappa_{lk}^{ac} - g_{i\widetilde{l}\widetilde{ck}}\ {}^t\kappa_{lk}^{ac}). \tag{47}$$

κ_{ij}^{ab} and ${}^t\kappa_{ij}^{ab}$ are two different combinations of the MP2 correlation coefficients from Eq. (28). They are given as

$$\kappa_{ij}^{ab} = \kappa_{ij}^{ab}(1) + \sqrt{3}\kappa_{ij}^{ab}(2) \tag{48}$$

$${}^t\kappa_{ij}^{ab} = \kappa_{ij}^{ab}(1) - \frac{1}{\sqrt{3}}\kappa_{ij}^{ab}(2) = \frac{1}{3}(\kappa_{ij}^{ab} + 2\kappa_{ij}^{ba}). \tag{49}$$

Another second order contribution originates from taking two first order wave functions together with the Fock operator, F. This contribution is very simple if one works with canonical orbitals. In that case, the singlet and triplet elements are the same

$$-\langle 0^{(1)}|\left[q_{ia}, \left[\sum_{bj} (b_{bj}^{ph}q_{bj}^\dagger + b_{jb}^{hp}q_{jb}), F\right]\right]|0^{(1)}\rangle = \sum_b (\epsilon_b - \epsilon_i)\rho_{ba}^{(2)}b_{bi}^{ph} + \sum_j (\epsilon_j - \epsilon_a)\rho_{ij}^{(2)}b_{aj}^{ph}, \tag{50}$$

$$-\langle 0^{(1)}|\left[q_{ia}^\dagger, \left[\sum_{bj} (b_{bj}^{ph}q_{bj}^\dagger + b_{jb}^{hp}q_{jb}), F\right]\right]|0^{(1)}\rangle = \sum_b (\epsilon_b - \epsilon_i)\rho_{ab}^{(2)}b_{ib}^{hp} + \sum_j (\epsilon_j - \epsilon_a)\rho_{ji}^{(2)}b_{ja}^{hp}. \tag{51}$$

The linear transformations with the overlap matrix, $\mathbf{S}^{[2]}$, must also be taken through second order, and again the singlet and triplet cases are the same

$$(\mathbf{S}^{[2]}\mathbf{b})_{ai} = \sum_{jb} \begin{pmatrix} \langle 0^{(1)}|[E_{ia}^S, & b_{bj}^{ph}E_{bj}^S]|0^{(1)}\rangle \\ \langle 0^{(1)}|[E_{ai}^S, & b_{jb}^{hp}E_{jb}^S]|0^{(1)}\rangle \end{pmatrix} = \begin{pmatrix} {}^1m_{ai} \\ {}^2m_{ia} \end{pmatrix} \tag{52}$$

where

$${}^1m_{ai} = \sum_j b_{aj}^{ph}\rho_{ij}^{(2)} - \sum_b \rho_{ba}^{(2)}b_{bi}^{ph}, \tag{53}$$

$${}^2m_{ia} = \sum_b b_{ib}^{hp}\rho_{ab}^{(2)} - \sum_j \rho_{ji}^{(2)}b_{ja}^{hp}. \tag{54}$$

We can see that the terms entering in the direct linear transformation with the overlap matrix, $\mathbf{S}^{[2]}$, are very similar to those encountered in Eqs. (50) and (51) for the Fock operator. Equations (43), (50), and (52) define the HRPA approximation. This is not a particularly accurate method. It gives excitation energies which are generally too large and accordingly underestimates response properties.[28] These deficiencies arise from the absence of $2p-2h$ renormalization terms. The wavefunction is extended to second order, as with SOPPA, but the $2p-2h$ excitations are neglected. In order to improve on this method, it is therefore necessary to introduce renormalization via the $2p-2h$ manifold.

The contributions to the $2p-2h$ block of $\mathbf{E}^{[2]}b$ coming from the first vector in Eq. (29) involve the doubly excited states $|\mu^S\rangle$. They can be evaluated as

$$\sum_{kc}\begin{pmatrix} b^{ph}_{ck}C^S_{iajb,ck}(I) \\ b^{hp}_{kc}C^S_{aibj,kc}(I)\end{pmatrix}=-\begin{pmatrix} \langle\mu^S(I)|H^S(b)|HF\rangle \\ -\langle HF|H^S(b)|\mu^S(I)\rangle\end{pmatrix}, \quad (55)$$

where

$$-\langle\mu^+(1)|H^+(b)|HF\rangle = \frac{1}{\sqrt{(1+\delta_{ij})(1+\delta_{ab})}}(g_{\tilde{i}a\tilde{j}b}+g_{ia\tilde{j}\tilde{b}}+g_{\tilde{i}\tilde{b}ja}+g_{ib\tilde{j}\tilde{a}}), \quad (56)$$

$$-\langle\mu^+(2)|H^+(b)|HF\rangle = \sqrt{3}(g_{\tilde{i}a\tilde{j}b}+g_{ia\tilde{j}\tilde{b}}-g_{\tilde{i}\tilde{b}ja}-g_{ib\tilde{j}\tilde{a}}), \quad (57)$$

$$-\langle\mu^-(1)|H^-(b)|HF\rangle = \sqrt{3}(g_{\tilde{i}a\tilde{j}b}+g_{ia\tilde{j}\tilde{b}}-g_{\tilde{i}\tilde{b}ja}-g_{ib\tilde{j}\tilde{a}}), \quad (58)$$

$$-\langle\mu^-(2)|H^-(b)|HF\rangle = \frac{1}{\sqrt{1+\delta_{ab}}}(g_{\tilde{i}a\tilde{j}b}-g_{ia\tilde{j}\tilde{b}}+g_{\tilde{i}\tilde{b}ja}-g_{ib\tilde{j}\tilde{a}}), \quad (59)$$

$$-\langle\mu^-(3)|H^-(b)|HF\rangle = \frac{1}{\sqrt{1+\delta_{ij}}}(g_{\tilde{i}a\tilde{j}b}-g_{ia\tilde{j}\tilde{b}}-g_{\tilde{i}\tilde{b}ja}+g_{ib\tilde{j}\tilde{a}}), \quad (60)$$

where the transformed integrals are defined in Eqs. (33) and (34). The terms in the second line of Eq. (55) can be found from the above by replacing all g_{pqrs} with g_{qpsr}, for example

$$\langle HF|H^+(b)|\mu^+(1)\rangle = \frac{1}{\sqrt{(1+\delta_{ij})(1+\delta_{ab})}}(g_{\tilde{a}i\tilde{b}j}+g_{ai\tilde{b}\tilde{j}}+g_{\tilde{b}i\tilde{a}j}+g_{bi\tilde{a}\tilde{j}}). \quad (61)$$

2. Contributions from the $2p-2h$ trial vector

The $2p-2h$ corrections are introduced via the trial vectors $\mathbf{b}^{2p2h}$. Following the definition of SOPPA and the conclusions reached in Sec. II B, we evaluate terms involving both $p-h$ and $2p-2h$ excitations to first order and terms involving only the $2p-2h$ excitations to zeroth order. Returning to Eq. (29), we are now interested in the $\mathbf{E}^{[2]}\mathbf{b}^{2p2h}$ transformation,

$$[\mathbf{E}^{[2]}\mathbf{b}^{2p2h}]_\mu=-\begin{pmatrix} \langle 0|[q_\mu,H]|0^R\rangle \\ \langle\mu^S|H|0^R\rangle \\ \langle 0^L|[q^\dagger_\mu,H]|0\rangle \\ -\langle 0^L|H|\mu^S\rangle\end{pmatrix}. \quad (62)$$

The states $|\mu^S\rangle$ and $|0^R\rangle$, $\langle 0^L|$ are either singlet or triplet. The first and third rows of this vector are very similar to the expression in Eq. (43). The correlation coefficients, κ, are replaced by a $2p-2h$ trial vector, and the one-index transformed Hamiltonian is replaced by the normal Hamiltonian. We therefore expect these terms to be very similar, and indeed they are. Note that in Eq. (48), the correlation coefficients that are used are combinations of the singlet–singlet and triplet–triplet spin-coupled singlet $2p-2h$ excitation operators, which gives the simple expressions in Eqs. (44) and (45). In the singlet case we get

$$\sum_{I=1,2}\sum_{\substack{a\geqslant b\\ i\geqslant j}}\begin{pmatrix} b^{2p2h}_{aibj}(I)C^+_{aibj,kc}(I) \\ b^{2h2p}_{iajb}(I)C^+_{iajb,ck}(I)\end{pmatrix} = -\begin{pmatrix} \langle HF|[E^+_{kc},H]|0^R\rangle \\ \langle 0^L|[E^+_{ck},H]|HF\rangle\end{pmatrix} \quad (63)$$

and in the triplet case

$$\sum_{I=1,3}\sum_{\substack{a\geqslant b\\ i\geqslant j}}\begin{pmatrix} b^{2p2h}_{aibj}(I)C^-_{aibj,kc}(I) \\ b^{2h2p}_{iajb}(I)C^-_{iajb,ck}(I)\end{pmatrix} = -\begin{pmatrix} \langle HF|[E^-_{kc},H]|0^R\rangle \\ \langle 0^L|[E^-_{ck},H]|HF\rangle\end{pmatrix}. \quad (64)$$

The full expressions for the $\mathbf{C}^S(I)$ matrices can be found in the Appendix. Using the $\mathbf{C}^+$ matrices of Eqs. (A1) and (A2) the linear transformation reads

$$\begin{aligned}-\langle HF|[E^+_{kc},H]|0^R\rangle &= \sum_{\substack{a\geqslant b\\ i\geqslant j}}\frac{b^{2p2h}_{aibj}(1)}{\sqrt{(1+\delta_{ij})(1+\delta_{ab})}}(\delta_{ki}(g_{cajb}+g_{cbja}) \\ &+\delta_{kj}(g_{cbia}+g_{caib})-\delta_{ac}(g_{ikjb}+g_{ibjk})-\delta_{bc}(g_{jkia} \\ &+g_{jaik}))+\sum_{\substack{a>b\\ i>j}}\sqrt{3}b^{2p2h}_{aibj}(2)(\delta_{ki}(g_{cajb}-g_{cbja}) \\ &+\delta_{kj}(g_{cbia}-g_{caib})-\delta_{ac}(g_{ikjb}-g_{ibjk}) \\ &-\delta_{bc}(g_{jkia}-g_{jaik})) \\ &=\sum_{bj}\left(\sum_a {}^sb^{2p2h}_{akbj}g_{cajb}-\sum_i {}^sb^{2p2h}_{cibj}g_{ikjb}\right), \end{aligned} \quad (65)$$

where

$${}^sb^{2p2h}_{aibj}=\sqrt{(1+\delta_{ij})(1+\delta_{ab})}\ {}^sb^{2p2h}_{aibj}(1) + \mathrm{sgn}((a-b)(i-j))\sqrt{3}\ {}^sb^{2p2h}_{aibj}(2). \quad (66)$$

The expression in Eq. (65) is obtained by changing the restricted summation to a free summation over the involved indices and using the symmetry in the trial vectors. We have used the sign function, $\mathrm{sgn}(p)$, defined as

$$\mathrm{sgn}(p)=\begin{cases} 1 & \text{if } p>0 \\ 0 & \text{if } p=0 \\ -1 & \text{if } p<0\end{cases}. \quad (67)$$

Similarly using the $\mathbf{C}^-$ matrices of Eqs. (A3)–(A5) we obtain

$$-\langle HF|[E^{-}_{kc},H]|0^R\rangle$$

$$=\sum_{bj}\left(\sum_{a}{}^{t}b^{2p2h}_{akbj}g_{cajb}-\sum_{i}{}^{t}b^{2p2h}_{cibj}g_{ikjb}\right) \tag{68}$$

with

$$\begin{aligned}{}^{t}b^{2p2h}_{aibj}=&\,\mathrm{sgn}((a-b)(i-j))\sqrt{2}b^{2p2h}_{aibj}(1)\\&+\mathrm{sgn}(i-j)\sqrt{1+\delta_{ab}}b^{2p2h}_{aibj}(2)\\&+\mathrm{sgn}(a-b)\sqrt{1+\delta_{ij}}b^{2p2h}_{aibj}(3).\end{aligned} \tag{69}$$

The final two terms required in Eq. (62) are the linear transformations with the $\mathbf{D}^{(0)}$ matrix of SOPPA. This transformation is straightforward, due to the simple diagonal form of the $\mathbf{D}^{(0)}$ matrix

$$\begin{aligned}D^{(0)}_{aibj,aibj}=&-\langle HF|[R_\mu,[R^\dagger_\mu,F]]|HF\rangle\\&=\epsilon_a+\epsilon_b-\epsilon_i-\epsilon_j,\end{aligned} \tag{70}$$

which is the same for all singlet and triplet $2p-2h$ excitations. Using the definitions of the doubly excited states, Eqs (38) and (39), the transformation for both singlet and the triplet cases can be seen to give

$$-\begin{pmatrix}\langle\mu(I)|H|0^R\rangle\\-\langle 0^L|H|\mu(I)\rangle\end{pmatrix}=\begin{pmatrix}b^{2p2h}_{aibj}(I)(\epsilon_a+\epsilon_b-\epsilon_i-\epsilon_j)\\b^{2h2p}_{iajb}(I)(\epsilon_a+\epsilon_b-\epsilon_i-\epsilon_j)\end{pmatrix}. \tag{71}$$

Finally, the $p-h$ – $2p-2h$ coupling block of the overlap matrix, $\mathbf{S}^{[2]}$, is zero when evaluated through first order. The diagonal elements of the $\mathbf{S}^{[2]}$ matrix in the $2p-2h$ part should be evaluated through zeroth order which gives simply a unit matrix.

This concludes the description of the linear transformations with all the propagator matrices on the trial vectors in Eq. (12). We have given sufficient details so that it should be possible to follow all steps of the procedure. Further information about the actual computational implementation may be obtained from the authors.[29]

Before proceeding with a couple of numerical applications of these equations we will discuss the iterative technique needed to determine excitation energies and response properties (Sec. II E) and we will also compare this implementation and the previous partitioned SOPPA method.

E. The iterative algorithm

One of the basic ideas of this implementation of the SOPPA equations is the use of direct ''matrix-times-trial-vector technique'' in order to avoid explicit constructions of the $\mathbf{E}^{[2]}$ and $\mathbf{S}^{[2]}$ matrices. Because of the paired structure of the matrices is the same in SOPPA and in the multiconfigurational linear response (MCLR) method we can use the variant of the conjugate gradient method[30] that was first applied to the MCLR problem by Olsen *et al.*[31] and Jørgensen *et al.*[21] The only modification of the equations that is needed is the replacement of the configurational trial vectors with the $2p-2h$ trial vectors.

We shall summarize the procedure in the case of the determination of the k lowest excitation energies. They are obtained from the solution of the equation

$$(\mathbf{E}^{[2]}-\omega_l\mathbf{S}^{[2]})X_l=0 \quad (l=1,2,\cdots k). \tag{72}$$

We may recast this equation into an equivalent form

$$(\mathbf{E}^{[2]}-\omega_l\mathbf{S}^{[2]})\mathbf{b}\tilde{\mathbf{b}}X_l=0 \tag{73}$$

provided $\mathbf{b}$ is a matrix in which the columns form a real orthonormal basis in the space spanning the ph, hp, $2p2h$, $2h2p$, etc., excitations. Premultiplying this equation by $\tilde{\mathbf{b}}$ shows that Eq. (73) is equivalent to solving the equation

$$(\mathbf{E}^{[2]R}-\omega_l\mathbf{S}^{[2]R})X^R_l=0, \tag{74}$$

where

$$\mathbf{E}^{[2]R}=\tilde{\mathbf{b}}\mathbf{E}^{[2]}\mathbf{b}=\tilde{\mathbf{b}}\mathbf{u}^R, \tag{75}$$

$$\mathbf{S}^{[2]R}=\tilde{\mathbf{b}}\mathbf{S}^{[2]}\mathbf{b}=\tilde{\mathbf{b}}\mathbf{m}^R, \tag{76}$$

and

$$X^R_l=\tilde{\mathbf{b}}X_l. \tag{77}$$

The columns of the $\mathbf{u}^R$ matrix correspond to the linear transformed trial vectors of either $p-h$ type, Eqs. (42), (44)–(47), (50), (51), and (56)–(61), or $2p-2h$ type, Eqs. (65)–(69), and (71), while the columns of the $\mathbf{m}^R$ matrix correspond to the ${}^1m$ and ${}^2m$ matrices defined in Eqs. (53) and (54) for $p-h$ type trial vectors and to the $2p-2h$ trial vectors in the $2p-2h$ subspace.

However, if the $\{b_l\}$ basis was incomplete then Eq. (73) would not be fulfilled and the solutions of Eqs. (72) and (74) would not be identical. The method of solution we apply consists of choosing a successively larger $\mathbf{b}$ basis set, i.e., adding more columns to $\mathbf{b}$, until Eqs. (72) and (74) are equivalent to within a given tolerance. The procedure is iterative and has the following steps:

(1) The initial guess on the basis, or trial, vectors $\mathbf{b}^{(0)}$ consists of k columns where in each column all elements but one in the particle–hole part are zero. The nonzero elements are chosen such that $\mathbf{b}^{(0)}$ is the solution to Eq. (72) in a diagonal approximation for the k lowest particle–hole excitations.

(2) The two-electron integrals in the molecular orbital basis are read into core serially as $(**|rs)$ distributions, and the one-index transformed integrals are constructed according to Eqs. (32)–(34). The contributions to $\mathbf{u}^R$ requiring integrals [Eqs. (42), (44)–(47), (56)–(61), and (65)–(69)] are constructed on the fly. This step represents by far the most time consuming part of the calculation. After all integrals have been read the remaining contributions to $\mathbf{u}^R$ and $\mathbf{m}^R$ are constructed.

(3) $\mathbf{E}^{[2]R}$ and $\mathbf{S}^{[2]R}$ are determined according to Eqs. (75) and (76), Eq. (74) is solved to obtain $X^{R(0)}_l$ and $\omega^{(0)}_l$, and $X^{(0)}_l$ is calculated from Eq. (77).

(4) If $X^{(0)}_l$ were the correct solution vector for the lth eigenvector it would also satisfy Eq. (72). However, if this is not the case then

TABLE I. Computational details of the calculations of the singlet spectrum of benzene.[a]

Symmetry[b]	A_g	B_{3u}	B_{2u}	B_{1g}	B_{1u}	B_{2g}	B_{3g}	A_u
Occupied orbitals	6	5	4	3	1	1	1	0
Virtual orbitals	26	25	19	20	11	11	7	7
b^{ph} [c]	22	16	15	22	25	16	16	19
b^{2p2h} [c]	21	16	16	21	19	12	12	17
Iterations[d]	20	8	8	20	18	7	7	17
Excitations[e]	480 992	479 668	478 372	478 373	397 432	397 433	396 179	396 178
Total timings[f]	4 142	2 053	1 940	4 140	3 674	1 490	1 601	2 934

[a]Using the ANO basis set of Ref. 18 consisting of 147 CGTO's. Four excitation energies are computed in each symmetry.
[b]In D_{2h} point group symmetry.
[c]Number of trial vectors of particle–hole (b^{ph}) and two-particle, two-hole (b^{2p2h}) type when the iteration process has converged.
[d]Number of iterations before solution vectors converge to 10^{-2} a.u., i.e., excitation energies to 10^{-4} a.u.
[e]Total number of excitations (ph and $2p2h$).
[f]Total timing for the full iterative process on a Silicon Graphics Inc. INDIGO^2 (150 MHz, R4400, 96 MB memory) in CPU seconds.

$$R_l^{(0)}=(\mathbf{E}^{[2]}-\omega_l^{(0)}\mathbf{S}^{[2]})X_l^{(0)}\neq 0 \tag{78}$$

or from Eq. (77) and the definition of the $\mathbf{u}^R$ and $\mathbf{m}^R$ matrices

$$R_l^{(0)}=(\mathbf{u}-\omega_l\mathbf{m})X_l^{R(0)}. \tag{79}$$

(5) For each $R_l^{(0)}$ larger than the specified tolerance we add an extra trial vector to the $\mathbf{b}^{(0)}$ matrix. The new basis vector is obtained from a diagonal approximation to Eqs. (72) and (79), that is

$$b_{k+1}^l=(\mathbf{E}^{[2]}-\omega_l^{(0)}\mathbf{S}^{[2]})_{\text{diag}}^{-1}R_l^{(0)} \tag{80}$$

which is an estimate of the error $X_l-X_l^{(0)}$. The new trial vector is either of the $p-h$ type or of the $2p-2h$ type and we base the choice on the magnitude of $R_l^{(0)}$ computed in the two individual subspaces.

(6) The $\mathbf{b}^{(1)}=(\mathbf{b}^{(0)},b_{k+1},\ldots,b_{k+p})$, where $p\leqslant k$, matrix is now used as the next guess on the complete basis set and we carry out the computational steps from (2)–(6) again. The iterative process stops when all R_l's $l=1,2,\cdots k$ are less than the specified tolerance.

The calculations reported in this paper are carried out on a Silicon Graphics Inc. INDIGO^2 workstation. More detailed informations on the benzene calculation is given in Table I. We see that the number of iterations needed vary from 7 to 20 in the eight D_{2h} irreducible representations. The largest number of iterations is typically needed in cases where the initial trial vectors do not include the most important excitations for the lowest roots.

Table I illustrates the computational efforts involved in determining four excitation energies (and oscillator strengths for allowed transitions) of each symmetry. However, since the extra basis vectors that are added to the basis set if a given R_l is larger than the threshold not only benefit the convergences in the space spanning X_l but also the other eigenvectors of the same symmetry we find that timing/root will decrease as we determine more roots of the same symmetry.

We see from Table I the number of iterations needed to converge the iterative procedure is larger than the number of occupied orbitals for all symmetries. Since one of the difference between this implementation of SOPPA and the previous ones is a reduction of operation count by N_O (number of occupied orbitals) we do not find any time saving for this test example when going from an N^6 to an iterative N^5 procedure. However, the number of excitations is so large that it would be impossible to construct the requisite matrices, especially those from the $2p-2h$ corrections, needed in the partitioned SOPPA implementations and the benzene calculation could therefore not be carried with the previous versions of SOPPA programs. Another point in favor of the present approach is that we can foresee that N_O becomes larger than the number of iterations for larger molecules and the present implementation will thus be computationally less demanding for larger systems.

A note on the disk space required in the iterative calculation may be in place. A large fraction of the total number of excitations are $2p2h$ excitations. In order avoid storing too many of them on disk we only save the ones that are needed in connection with two-electron integrals, i.e., in Eqs. (65)–(69). In the rest of the cases, see Eq. (71), we construct the elements as they are needed. The latter procedure is also applied to the construction of the $\mathbf{m}^R$ matrix. As a result of this strategy the calculation on benzene needed less than 600 MB of disk space.

F. Comparison with the partitioned version of SOPPA

It is worthwhile to stress the differences between this and previous implementations of SOPPA. When calculating the response through second order it is necessary, as discussed above, to include both the $p-h$ and the $2p-2h$ excitation operators. The practical effect of including the $2p-2h$ manifold is to make the propagator matrix of very large dimension, so that its explicit construction is not feasible. The original derivation of SOPPA[9] avoided this problem by partitioning the propagator matrix. The $2p-2h$ contributions were folded into the $p-h$ manifold, so that the matrix was of the same dimension as in RPA.

The partitioning gives a modified $p-h$ block of the propagator matrix. This partitioned $p-h$ matrix can be given as

$$\mathbf{P}=\mathbf{M}_{11}-\mathbf{M}_{12}\mathbf{M}_{22}^{-1}\mathbf{M}_{21}, \tag{81}$$

where the subscripts on **M** denotes the excitation level in each term. Thus $\mathbf{M}_{11}$ corresponds to the $\mathbf{A}^{(0,1,2)}$ and $\mathbf{B}^{(1,2)}$ matrices already defined, while $\mathbf{M}_{12}$ and $\mathbf{M}_{21}$ correspond to the $\mathbf{C}^{(1)}$ matrices. $\mathbf{M}_{22}^{-1}$ corresponds to the inverse of the $\mathbf{D}^{(0)}$ matrix. Nielsen *et al.*[9] have shown that we need only **P** through second order to obtain response properties to the same order. This gives us another way of determining the orders of the individual terms. If **P** is to be correct through second order, the same must be true for $\mathbf{M}_{11}$ and $\mathbf{M}_{12}\mathbf{M}_{22}^{-1}\mathbf{M}_{21}$. Thus $\mathbf{M}_{11}$ has to be correct through second order by itself, which is what we already know from our earlier order analysis. It is also clear that the $\mathbf{M}_{12}$ matrices have to be correct through first order, while the $\mathbf{M}_{22}$ matrix only has to be zeroth order. In the approach used here, the same orders were assigned to the **M** matrices, even though the partitioning is now unnecessary. Finally, the $\mathbf{W}_4$ matrix[10] which must be included in the response for the partitioned approach is included implicitly in the direct linear transformations. The implementation of SOPPA we have outlined in this paper gives response properties that are identical to those obtained in the partitioned approach. The present approach has two important advantages over the original implementation, however. The first is that the linear transforms allow for much larger $2p-2h$ manifolds, since the propagator matrix is never explicitly constructed and the second is that by using the one-index transformed integrals the operation count is decreased by one order to N^5 [Eqs. (43)–(47)]. However, the latter point will only be visible computationally when the number of iterations needed to converge the eigenvalue problem is less than the number of occupied orbitals.

III. RESULTS AND DISCUSSION

A prime motivation for this implementation is that it enables us to study larger molecular systems than has been previously possible. In this section we will therefore report calculations on benzene and naphthalene. These molecules have been widely studied using other methods, since they are representative of a wide class of aromatic compounds. We compare our results to those obtained using the CASPT2 method,[7,8] for both singlet and triplet perturbations.[18,19] We concentrate on the singlet and triplet excitation energies and oscillator strengths, although the SOPPA implementation also includes response properties, which will be reported elsewhere.

It is appropriate to compare SOPPA and CASPT2, since both methods include dynamic correlation effects via second-order perturbation theory. CASPT2 also includes nondynamic correlation through the multireference CAS space; it is capable of producing very accurate excitation spectra[32] and oscillator strengths. Although we cannot expect SOPPA to give such accurate results, given that it does not incorporate nondynamic correlation, it should be capable of giving consistent excitation spectra.

The CASPT2 approach has been shown to give excitation energies of good accuracy for a number of aromatic systems.[32] This provides us with a set of benchmark results. In order to facilitate the comparison, we have employed the same basis sets and geometries as those used by Roos and co-workers. In the case of benzene,[18] the basis set is of ANO type with C[4*s*3*p*1*d*]/H[2*s*1*p*], supplemented by [1*s*1*p*1*d*] diffuse functions located at the center of the molecule. This gives a total of 147 CGTO's. For naphthalene[19] the basis set is also of ANO type, consisting of C[3*s*2*p*1*d*]/H[2*s*], supplemented with [2*s*2*p*] functions located at the center of the molecule; this gives a total of 164 CGTO's. This corresponds to the BS5 basis set defined by Rubio *et al.*[19] The diffuse orbitals at the molecular center are designed to give a better description of Rydberg excitations; these excitations typically have large contributions from the diffuse virtual orbitals and this is how we have identified them. However, in order to describe Rydberg excitations into 3*d* orbitals, it is necessary to include two diffuse *d* functions. This then gives the BS6 basis set of Rubio *et al.*[19] Thus following these authors, we report BS5 basis set results for all naphthalene excitations except $2\ ^1B_{1u}$, $3\ ^1B_{2u}$ and $3\ ^1B_{3u}$, for which we use the BS6 basis set. The naphthalene basis set is clearly inferior to that of benzene, which will be reflected in the results. The calculations were performed with the HERMIT-SIRIUS-RESPONS program package.[21,22,33,34] These programs including the SOPPA implementation described in this paper will be part of the new quantum chemical program DALTON, which is scheduled for release on 1/1/97.

There have been numerous experimental studies of the excitation spectra of both benzene and naphthalene. We have followed the assignments made by Lorentzon *et al.*[18] for benzene and by Rubio *et al.*[19] for naphthalene. We therefore

TABLE II. Singlet excitation energies (eV) of benzene in ascending order of SOPPA energies.

State	CASSCF Ref. 18	CASPT2 Ref. 18	RPA This work	SOPPA This work	Expt.[g]
		Valence $^1\pi\pi^*$			
$1\ ^1B_{2u}$	4.80	4.84	5.82	4.69	4.90[a]
$1\ ^1B_{1u}$	7.32	6.30	5.88	6.01	6.20[a]
$1\ ^1E_{1u}$	8.53	7.03	7.50	6.75	6.94[b]
		Rydberg $^1\pi\pi^*$			
$2\ ^1E_{1u}$	6.46	7.16	7.16	7.03	7.41[b]
$1\ ^1E_{2g}$	7.09	7.77	7.80	7.55	7.81[d]
$2\ ^1A_{1g}$	7.14	7.74	7.77	7.56	7.81[c]
$1\ ^1A_{2g}$	7.08	7.81	7.85	7.59	7.81[c]
		Rydberg $^1\pi\sigma^*$			
$1\ ^1E_{1g}$	6.26	6.38	6.54	6.18	6.33[e]
$1\ ^1A_{2u}$	6.66	6.86	6.94	6.70	6.93[f]
$1\ ^1E_{2u}$	6.74	6.91	7.11	6.76	6.95[f]
$1\ ^1A_{1u}$	6.82	6.99	7.28	6.83	
$2\ ^1E_{1g}$	7.33	7.57	7.59	7.34	7.54[d]
$1\ ^1B_{2g}$	7.33	7.58	7.68	7.35	7.46[c]
$1\ ^1B_{1g}$	7.29	7.58	7.70	7.35	7.46[c]
$3\ ^1E_{1g}$	7.37	7.57	7.73	7.40	

[a]Reference 35.
[b]Reference 36.
[c]Reference 37.
[d]Reference 38.
[e]Reference 39.
[f]Reference 40.
[g]Experimental assignments from Ref. 18.

refer to these papers for details of the assignments and discussions of any uncertainties in the experimental data.

A. Benzene

The lowest 15 singlet–singlet excitation energies of benzene are listed in Table II. They have been divided into three groups, according to the designations of Lorentzon *et al.*[18] The energies have been placed in ascending order with respect to SOPPA, although only the CASSCF results show a significantly different ordering. The largest difference between SOPPA and CASPT2 is 0.29 eV, for the $1\,^1B_{1u}$ excitation, with most being in much closer agreement. The agreement between RPA and CASPT2 is similar to that for SOPPA. However, the SOPPA values are all less than CASPT2, while those from RPA are not.

The three valence $^1\pi\pi^*$ excitations are given to within 0.21 eV of experiment by SOPPA, which is consistently better than RPA. The $2\,^1E_{2g}$ excitation is not included in Table II. In CASPT2 this excitation is also predicted to be low-lying with a value of 7.90 eV, while we obtain 10.35 eV in RPA and 8.52 in SOPPA. Lorentzon *et al.*[18] note that this state has significant double excitation character, which explains why SOPPA fails to describe this excitation. CASPT2 performs better than SOPPA for these states, with errors of no more than 0.1 eV. However, the SOPPA excitation energies are all below the experimental values, in contrast to RPA or the two CAS methods. The poor performance of CASSCF, especially for $1\,^1E_{1u}$ and $1\,^1B_{1u}$, indicates the importance of dynamic correlation effects in this system.

The $^1\pi\pi^*$ Rydberg excitations ($2\,^1A_{1g}$, $1\,^1E_{2g}$, and $1\,^1A_{2g}$) are of similar energy. Both CASPT2 and RPA give results in close agreement with experiment, while the SOPPA values are again around 0.25 eV in error. The $2\,^1E_{1u}$ experimental excitation energy is significantly larger than that given by either CASPT2 or SOPPA. For the Rydberg $^1\pi\sigma^*$ excitations, CASPT2 is generally in excellent agreement with experiment, while SOPPA and CASSCF are in error by no more than 0.21 eV. SOPPA again consistently underestimates the experimental values.

The CASSCF results show a much larger error for the $^1\pi\pi^*$ Rydberg states than the $^1\pi\sigma^*$ states. Lorentzon *et al.*[18] suggest that this indicates a systematic difference in the dynamic correlation contribution to these states. We do not see any evidence for this from SOPPA, however, since the difference between theory and experiment is around 0.2 eV for all of these excitations.

The ANO basis set used for the Rydberg states is not completely converged. A basis set investigation shows that the remaining basis set effect increases the excitation energy by around 0.2 eV for these states.[41]

The lowest 16 singlet–triplet excitation energies of benzene are listed in Table III. They have again been divided into three groups, although there are experimental values for the valence excitations only. There is good agreement between experiment and both SOPPA and CASPT2, although both give rather low estimates for the $1\,^3E_{1g}$ excitation. The SOPPA results are again consistently below the experimental values. There is a large error in the CASSCF result for $1\,^3E_{2u}$, which has been related to the ionic nature of this excitation.[18] RPA has a triplet instability for the $1\,^3E_{1u}$ excitation; such instabilities are commonly encountered in this method.[10] No experimental values are available for the Ryd-

TABLE III. Singlet–triplet excitations of benzene (eV) in ascending order of SOPPA energies.

State	CASSCF Ref. 18	CASPT2 Ref. 18	RPA (This work)	SOPPA (This work)	Expt.[c]
			Valence $^3\pi\pi^*$		
$1\,^3B_{1u}$	4.05	3.89	Instability	3.75	3.94[a]
$1\,^3E_{1u}$	5.07	4.49	4.70	4.48	4.76[a]
$1\,^3B_{2u}$	6.93	5.49	5.07	5.50	5.60[a]
$1\,^3E_{2g}$	7.61	7.12	7.24	7.41	7.24–7.74[b]
			Rydberg $^3\pi\pi^*$		
$2\,^3E_{1u}$	6.92	6.98	7.11	6.92	
$2\,^3E_{2g}$	7.44	7.55	7.85	7.57	
$1\,^3A_{2g}$	7.50	7.70	7.85	7.59	
$1\,^3A_{1g}$	7.42	7.62	7.64	7.50	
			Rydberg $^3\pi\sigma^*$		
$1\,^3E_{1g}$	6.22	6.34	6.44	6.14	
$1\,^3A_{2u}$	6.61	6.80	6.82	6.64	
$1\,^3E_{2u}$	6.73	6.90	7.08	6.74	
$1\,^3A_{1u}$	6.83	7.00	7.28	6.84	
$2\,^3E_{1g}$	7.31	7.57	7.51	7.32	
$1\,^3B_{2g}$	7.27	7.53	7.65	7.33	
$1\,^3B_{1g}$	7.27	7.53	7.69	7.35	
$3\,^3E_{1g}$	7.36	7.56	7.71	7.38	

[a]Reference 42.
[b]See Ref. 18.
[c]Experimental assignments from Ref. 18.

TABLE IV. Singlet excitations in naphthalene (eV), in ascending order of SOPPA energies. The *R* in parenthesis indicates a Rydberg excitation.

State	CASSCF Ref. 19	CASPT2 Ref. 19	RPA (This work)	SOPPA (This work)	Expt.[d]
$1\,^1B_{3u}$	4.36	4.03	5.02	3.86	4.0[a]
$1\,^1B_{2u}$	6.51	4.56	4.80	4.44	4.70[a]
$1\,^1A_u(R)$	5.58	5.54	5.76	5.36	5.6[a]
$2\,^1A_g$	5.86	5.39	6.88	5.55	5.52[b]
$1\,^1B_{1g}$	6.62	5.53	6.21	5.64	5.22[b]
$2\,^1B_{3u}$	7.99	5.54	6.57	5.68	5.89[a]
$1\,^1B_{2g}(R)$	5.88	5.94	6.13	5.78	
$1\,^1B_{3g}(R)$	5.94	5.98	6.20	5.81	
$2\,^1B_{2u}$	7.95	5.93	6.67	5.87	6.0[a]
$1\,^1B_{1u}(R)$	5.90	6.03	6.45	5.97	
$2\,^1B_{1g}$	8.44	5.87	6.61	6.08	5.8[c]
$3\,^1B_{1g}(R)$	6.04	6.08	7.14	6.34	
$2\,^1B_{2g}(R)$	6.26	6.45	6.86	6.38	
$2\,^1B_{1u}(R)$	6.37	6.50	6.73	6.39	
$2\,^1B_{3g}(R)$	6.25	6.48	6.95	6.42	
$3\,^1B_{2u}(R)$	7.26	6.67	6.84	6.55	
$2\,^1A_u(R)$			6.87	6.56	
$3\,^1B_{3u}(R)$	7.41	6.58	6.86	6.57	
$3\,^1A_g$	7.05	6.04	7.15	6.63	6.05[b]
$4\,^1A_g(R)$	6.75	6.76	7.80	6.86	
$4\,^1B_{2u}$	10.23	7.16	8.77	7.71	7.6[a]

[a]Reference 43.
[b]Reference 44.
[c]Reference 45.
[d]Experimental assignments from Ref. 19.

berg excitations, but both SOPPA and RPA are within 0.2 eV of CASPT2 for all but two RPA values, so it is difficult to say which performs better.

B. Naphthalene

The naphthalene singlet–singlet excitations are given in Table IV. We have indicated the Rydberg excitations, which generally correspond with those identified by Rubio *et al.*[19] The excitations are again listed in ascending order for SOPPA, but in contrast to benzene, there are several differences in the energy ordering in CASPT2 relative to SOPPA. With the exception of two states, our SOPPA results are all within 0.2 eV of CASPT2.

The two lowest excitations are of $^1B_{3u}$ and $^1B_{2u}$ symmetry and are described well in SOPPA, being within 0.14 and 0.24 eV of experiment, respectively. The CASSCF results show a large error, so it is clear that dynamic correlation effects are important for these states. The next SOPPA excitation is the Rydberg $1\,^1A_u$. CASPT2, by contrast, predicts that $2\,^1A_g$ is the third state. The reason for this reversal in the ^1A_g and ^1A_u states in SOPPA is not clear. Since the $1\,^1A_u$ is a Rydberg excitation, it may be that the diffuse Rydberg functions are inadequate to describe it properly. Certainly, the RPA result is closer to the experimental value of 5.6 eV than is SOPPA. The SOPPA valence $2\,^1A_g$ excitation, however, is very close to the experimental result.

The SOPPA $1\,^1B_{1g}$ and $2\,^1B_{3u}$ excitations are within 0.14 eV of the CASPT2 values, although both methods show poor agreement with the experimental $^1B_{1g}$ energy. The orderings of the six excitations between $1\,^1B_{2g}(R)$ and $3\,^1B_{1g}(R)$ vary for the different methods. Experimental values are available for the valence excitations, $2\,^1B_{2u}$ and $2\,^1B_{1g}$, for which CASPT2 is less than 0.1 eV error, while SOPPA is only within 0.3 eV of experiment. The $1\,^1B_{1u}(R)$ is a $(1a_u \rightarrow 3s)$ Rydberg state, for which SOPPA and CASPT2 are in close agreement. However, for the $(1a_u \rightarrow 3p_\sigma)$ Rydberg states, $1\,^1B_{2g}(R)$ and $1\,^1B_{3g}(R)$, which are part of the $n=3$ Rydberg series, there is a systematic difference between SOPPA and CASPT2.

A further Rydberg series follows the $2\,^1B_{1g}$ excitation. These $(1a_u \rightarrow 3p_\pi)$ states $[3\,^1B_{1g}(R)$, $2\,^1B_{2g}(R)$, and $2\,^1B_{3g}(R)]$ are very close to one another in energy, but have not been unambiguously identified in experimental spectra.[19] In SOPPA there is then another Rydberg state $[2\,^1A_u(R)]$, which is not listed by Rubio *et al.*[19] This is of $(1a_u \rightarrow 3s)$ type. The appearance of this excitation in the SOPPA spectrum mirrors that of the $1\,^1A_u(R)$ state, which is also of much lower energy than is found by CASPT2.

There is a large discrepancy between SOPPA and CASPT2 for the $3\,^1A_g$ state. While CASPT2 gives 6.04 eV, SOPPA has 6.63 eV (the experimental value is 6.05 eV). This is possibly due to the fact that the CASSCF $3\,^1A_g$ state has equal single and double excitation character. Such states cannot be described accurately within the SOPPA approximation. This point is further underlined by the $4\,^1A_g(R)$ excitation, for which there is much closer agreement. The $3\,^1B_{2u}(R)$ excitation involves the $3d$ diffuse orbitals. Its SOPPA value is close to CASPT2. $4\,^1B_{2u}$ is a valence state. This can clearly be seen from the oscillator strengths (Table VI), which are 0.8 for CASPT2 and 0.3 for SOPPA.

TABLE V. Singlet–triplet excitations in naphthalene (eV) in ascending order of SOPPA energies.

State	CASSCF Ref. 19	CASPT2 Ref. 19	RPA (This work)	SOPPA (This work)	Expt.[d]
$1\,^3B_{2u}$	3.24	3.04	Instability	2.77	
$1\,^3B_{3u}$	3.24	3.84	3.67	3.68	
$1\,^3B_{1g}$	4.49	4.18	2.32	4.02	4.33[a]
$2\,^3B_{2u}$	4.59	4.24	Instability	4.12	
$2\,^3B_{3u}$	4.73	4.40	4.43	4.56	
$1\,^3A_g$	5.64	5.22	4.57	4.97	5.25[b]
$2\,^3B_{1g}$	8.04	5.65	6.26	5.86	6.12[c],6.0[a]
$3\,^3B_{1g}$	6.91	6.18	6.95	6.13	
$2\,^3A_g$	8.15	5.77	6.39	6.14	
$3\,^3A_g$	6.68	5.85	6.94	6.37	5.93[b]

[a]Reference 46.
[b]Reference 47.
[c]Reference 48.
[d]Experimental assignments from Ref. 19.

The excitation spectra for SOPPA and CASPT2 clearly do not agree as well as for benzene. As we have noted, although the two lowest excitations are similar, the $^1A_u(R)$ states seem to be of much lower energy in SOPPA. Since both involve excitations into the diffuse s-type Rydberg orbitals, this inconsistency might be removed by using a larger set of Rydberg basis functions.

The naphthalene singlet–triplet excitations are given in Table V. Since SOPPA can give only the singlet–triplet spectrum, the CASPT2, CASSCF, and experimental triplet–triplet values have been corrected for the lowest singlet–triplet excitation, which is given as 3.0 eV from experiment[49] and 3.04 and 3.24 eV from CASPT2 and CASSCF, respectively.[19]

There are two triplet instabilities in the RPA spectrum, both of which are of $^3B_{2u}$ symmetry. The SOPPA energies are within 0.3 eV of the lowest three experimental energies, with less good agreement for the $3\,^3A_g$ state. The agreement between SOPPA and CASPT2 is also within 0.3 eV, except for the $2\,^3A_g$ and $3\,^3A_g$ states. The discrepancy for the ^3A_g states cannot be put down to their doubly-excited character, since $2\,^3A_g$ is predominantly singly excited.

C. Oscillator strengths

The singlet dipole-allowed oscillator strengths for benzene and naphthalene are listed in Table VI. We have given only those results for which comparison can be made to either CASPT2 or experiment. It is notable that for benzene, the length and velocity representations give almost equal oscillator strengths, while for naphthalene this is not the case. The two representations will give the same result for a complete basis, so we appear to have a more complete set for benzene than for naphthalene.

For benzene, the SOPPA $1\,^1E_{1u}$ oscillator strength lies at the lower end of the experimental range. There are no

TABLE VI. Oscillator strengths for singlet dipole-allowed transitions in benzene and naphthalene, in length (L) and velocity (V) representations.

	RPA		SOPPA		CASSCF/CASPT2	
	This work				Refs. 18 and 19	
State	L	V	L	V	L	Expt.[d]
			Benzene			
$1\,^1E_{1u}$	0.61	0.63	0.51	0.61	0.82	0.6–1.1[a]
$2\,^1E_{1u}$	0.11	0.12	0.11	0.14	0.058	
$1\,^1A_{2u}$	0.069	0.071	0.062	0.063	0.052	
			Naphthalene			
$1\,^1B_{3u}$	$3.6\cdot10^{-5}$	$5.1\cdot10^{-5}$	$8.6\cdot10^{-6}$	$2.6\cdot10^{-5}$	0.0004	0.002[b]
$1\,^1B_{2u}$	0.041	0.048	0.055	0.100	0.0496	0.1[b]
$2\,^1B_{3u}$	1.62	1.66	1.25	1.62	1.34	1.3[b]
$2\,^1B_{2u}$	0.427	0.450	0.223	0.304	0.31	
$1\,^1B_{1u}$	0.023	0.019	0.016	0.014	0.003	
$2\,^1B_{1u}$	0.011	0.0062	0.013	0.0085	0.0069	
$3\,^1B_{2u}$	0.037	0.029	0.0058	0.0028	0.0017	
$3\,^1B_{3u}$	0.085	0.10	0.0048	0.010	0.0176	
$4\,^1B_{2u}$	0.124	0.092	0.309	0.313	0.8481	0.8[c]

[a]Reference 18.
[b]Reference 50.
[c]Reference 51.
[d]Experimental assignments from Ref. 18 (benzene) and Ref. 19 (naphthalene).

other experimental results available for benzene. The other two SOPPA values listed are of the same order of magnitude as for CASPT2. For naphthalene, the SOPPA $1\,^1B_{3u}$ oscillator strength is an order of magnitude less than the experimental and CASPT2 values, while for the $1\,^1B_{2u}$ excitation, only the length form agrees well with CASPT2. The SOPPA length value for $2\,^1B_{3u}$ lies within the experimental range. The variation in the length and velocity values for naphthalene indicates that the basis set is not saturated with respect to these properties.

D. Summary

Our results indicate that SOPPA can provide excitation energies which in most cases are within 0.2 eV of experiment, for relatively large molecular systems such as benzene and naphthalene. We have also seen that SOPPA can usually give excitation energies which are within 0.2 eV of the CASPT2 method, when using identical basis sets. We find this encouraging, considering that CASPT2 is a multireference second-order theory. In those cases where there is significant disagreement between CASPT2 and SOPPA, the problem can usually be traced to the doubly excited nature of the excited state, which SOPPA is not able to treat adequately. The oscillator strengths are of the same order of magnitude in the two methods. In Figs. 1 and 2, we plot the percentage deviation of the calculated singlet excitation energies from the experimental values, for benzene and naphthalene, respectively. These figures clearly demonstrate that the trends in CASPT2 and SOPPA are similar, although CASPT2 is rather more accurate. They also point up the large variations which we see for CASSCF and RPA, particularly for the valence excitations.

Although the RPA Rydberg excitation energies are quite accurate for benzene, there are many other cases where the RPA result differs by over 1 eV from the correlated methods or from experiment. However, the most serious problem with RPA is encountered in the occasional appearance of triplet instabilities, typically in aromatic and conjugated hydrocarbons. In addition to this, the excitation energies vary between being greater than or less than experiment and so could not be used with any confidence to assign a spectrum. A similar observation applies to the CASSCF values which we have quoted.[18,19] The CASSCF results differ by up to 3 eV from CASPT2. The overall performance of SOPPA, relative to CASSCF, indicates clearly the importance of including dynamic correlation in order to describe excitation processes.

IV. CONCLUSIONS

We have reimplemented the SOPPA method, and thereby obtained a program that is much more efficient than the previous implementations, RPAC[13] and MUNICH.[14] We have used a direct linear transformation approach, which leads to a reduction in the operation count from N^6 to N^5. We are now able to use a much larger $2p-2h$ space so that we can study larger molecular systems and use more extended basis sets. We have demonstrated the potential of this implementation by applying it to singlet and triplet properties of benzene and naphthalene.

We can identify several advantages and disadvantages of using CASPT2, rather than SOPPA, for the calculation of excited state properties. Among the advantages are the inclusion of nondynamic correlation and the ability to treat doubly excited and open-shell states. Among the disadvantages are its greater cost, since each excited state must be optimized separately, and the presence of intruder states, especially for Rydberg excitations.[18] There is also the question of selecting the CAS space. This provides flexibility for optimizing the molecular wave function, but makes it difficult to apply to

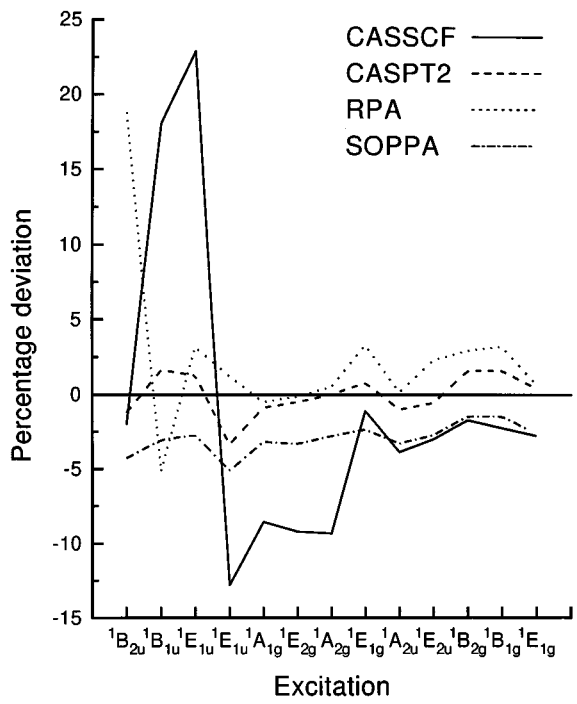

FIG. 1. Percentage deviation from experiment of the benzene singlet excitation energies. Energies are arranged in the same order as Table I.

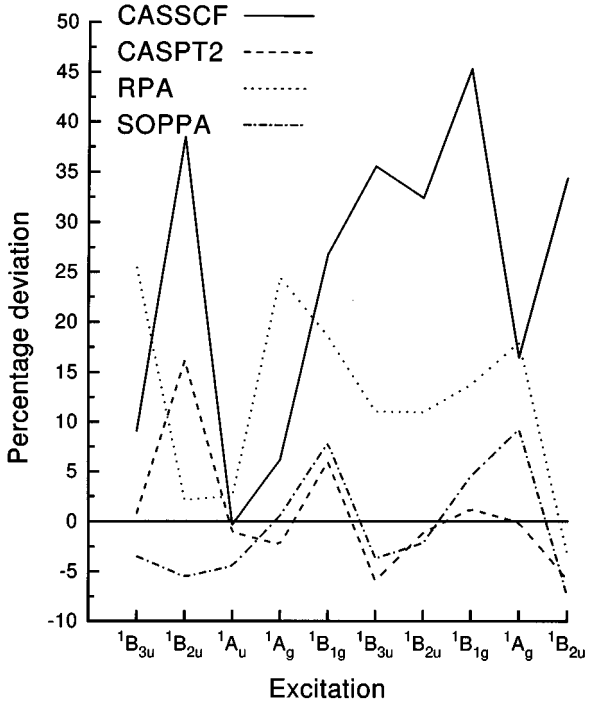

FIG. 2. Percentage deviation from experiment of the naphthalene singlet excitation energies. Energies are arranged in the same order as Table III.

general problems. In the case of benzene, for example, it was necessary to define different active spaces for the three types of excitations discussed.

Using the SOPPA approach, we cannot expect to obtain results of the accuracy of a multireference second-order method such as CASPT2. However, SOPPA has the advantage over multireference methods that, once the basis set has been selected, it is essentially a ''black-box'' approach. This means that it could be practical for chemists who do not specialize in theoretical methods. It will also give the entire excitation spectrum in a single calculation, since there is no need to optimize each excited state separately. An important caveat is that SOPPA is not able to describe doubly excited states. Therefore, if more accurate values are required for specific excitations, one should use CASPT2 or coupled-cluster based response methods. The SOPPA excitation spectrum, however, will generally be reliable; for the two molecules we have studied here, the excitation energies are within 0.2 eV of experiment, except for those states with appreciable doubly excited character. We would clearly need to study a larger set of molecules to investigate whether SOPPA can always give such agreement with experiment.

In this new implementation, the cost of a SOPPA calculation is comparable to that of an MP2 vibrational frequency calculation. In general, if the geometry and vibrational frequencies of a system can be obtained reliably at the MP2 level, one can expect that the excitation spectrum and response properties will be given reliably by SOPPA. We therefore recommend SOPPA as an accurate and efficient way to predict molecular properties at reasonable computational cost, for closed-shell systems.

ACKNOWLEDGMENTS

M.J.P. would like to thank the theoretical chemistry group in Odense for their hospitality during his stay and for providing such a lively and stimulating research environment. This research was supported by grants from the Danish Natural Science Research Council (Grant No. 11-0924 and Grant No. 93133141) and a Royal Society postdoctoral fellowship (M.J.P.).

APPENDIX A: THE C^S MATRICES

The $\mathbf{C}^+$ matrices, defined in Eq. (55), are given by Eqs. (C.16) and (C.17) of Ref. 10. [Equation (C.16) has an incorrect sign in Ref. 10.]

$$C^+_{iajb,ck}(1) = C^+_{aibj,kc}(1)$$
$$= \frac{1}{\sqrt{(1+\delta_{ij})(1+\delta_{ab})}} (\delta_{ik}(g_{cajb}+g_{cbja}) + \delta_{kj}(g_{cbia}+g_{caib}) - \delta_{ac}(g_{ikjb}+g_{ibjk}) - \delta_{bc}(g_{jkia}+g_{jaik})) \quad \text{(A1)}$$

and

$$C^+_{iajb,ck}(2) = C^+_{aibj,kc}(2)$$
$$= \sqrt{3}(\delta_{ik}(g_{cajb}-g_{cbja}) + \delta_{kj}(g_{cbia}-g_{caib}) - \delta_{ac}(g_{ikjb}-g_{ibjk}) - \delta_{bc}(g_{jkia}-g_{jaik})) \quad \text{(A2)}$$

and the C^- matrices by Eqs. (C.20), (C.21), and (C.22) of Ref. 10

$$C^-_{iajb,ck}(1) = C^-_{aibj,kc}(1) = \sqrt{2}(\delta_{ik}(g_{cajb} - g_{cbja}) + \delta_{kj}(g_{cbia} - g_{caib}) - \delta_{ac}(g_{ikjb} - g_{ibjk}) - \delta_{bc}(g_{jkia} - g_{jaik})), \tag{A3}$$

$$C^-_{iajb,ck}(2) = C^-_{aibj,kc}(2) = \frac{1}{\sqrt{1+\delta_{ab}}}(\delta_{ik}(g_{cajb} + g_{cbja}) + \delta_{kj}(g_{caib} + g_{cbia}) - \delta_{ac}(g_{ikjb} - g_{ibjk}) - \delta_{bc}(g_{jaik} - g_{jkia})), \tag{A4}$$

and

$$C^-_{iajb,ck}(3) = C^-_{aibj,kc}(3) = \frac{1}{\sqrt{1+\delta_{ij}}}(\delta_{ik}(g_{cajb} - g_{cbja}) + \delta_{kj}(g_{cbia} - g_{caib}) - \delta_{ac}(g_{ikjb} + g_{ibjk}) - \delta_{bc}(g_{jaik} + g_{jkia})). \tag{A5}$$

Due to our use of the E^S_{pq} operators rather than the normalized operators used in Ref. 10, these expressions are a factor of $\sqrt{2}$ larger than the corresponding expressions in Ref. 10.

[1] G. Maroulis, Mol. Phys. **74**, 131 (1991).
[2] R. Kobayashi, H. Koch, and P. Jørgensen, Chem. Phys. Lett. **219**, 30 (1994).
[3] C. Hattig and B. A. Hess, Chem. Phys. Lett. **233**, 359 (1995).
[4] F. Aiga, K. Sasagane, and R. Itoh, J. Chem. Phys. **99**, 3779 (1993).
[5] J. E. Rice and N. C. Handy, J. Chem. Phys. **94**, 4959 (1991).
[6] A. van der Avoird, P. E. S. Wormer, F. Mulder, and R. M. Berns, Topics Curr. Chem. **93**, 1 (1980).
[7] K. Anderson, P.-Å. Malmqvist, B. O. Roos, A. J. Sadlej, and K. Wolinski, J. Phys. Chem. **94**, 5483 (1990).
[8] K. Anderson, P.-Å. Malmqvist, and B. O. Roos, J. Chem. Phys. **96**, 1218 (1992).
[9] E. S. Nielsen, P. Jørgensen, and J. Oddershede, J. Chem. Phys. **73**, 6238 (1980).
[10] J. Oddershede, P. Jørgensen, and D. L. Yeager, Comput. Phys. Rep. **2**, 33 (1984).
[11] GAUSSIAN94, Revision B.2, M. J. Frisch, G. W. Trucks, H. B. Schlegel, P. M. W. Gill, B. G. Johnson, M. A. Robb, J. R. Cheeseman, T. Keith, G. A. Petersson, J. A. Montgomery, K. Raghavachari, M. A. Al-Laham, V. G. Zakrzewski, J. V. Ortiz, J. B. Foresman, J. Cioslowski, B. B. Stefanov, A. Nanayakkara, M. Challacombe, C. Y. Peng, P. Y. Ayala, W. Chen, M. W. Wong, J. L. Andres, E. S. Replogle, R. Gomperts, R. L. Martin, D. J. Fox, J. S. Binkley, D. J. Defrees, J. Baker, J. P. Stewart, M. Head-Gordon, C. Gonzalez, and J. A. Pople, Gaussian, Inc., Pittsburgh PA, 1995.
[12] Aa. E. Hansen and T. D. Bouman, Chem. Phys. Lett. **175**, 292 (1990).
[13] T. D. Bouman and Aa. E. Hansen, RPAC Molecular Properties Package, Version 9.0, Copenhagen University, Copenhagen, 1990.
[14] G. H. F. Diercksen and W. P. Kraemer, MUNICH reference manual, special technical report, Max-Planck-institut für Physik und Astrophysik, Munich, 1981.
[15] G. H. F. Diercksen, N. E. Grüner, and J. Oddershede, Comput. Phys. Commun. **30**, 349 (1983).
[16] J. Olsen and P. Jørgensen, J. Chem. Phys. **82**, 3235 (1985).
[17] B. O. Roos, K. Anderson, and M. P. Fülscher, Chem. Phys. Lett. **192**, 5 (1992).
[18] J. Lorentzon, P.-Å. Malmqvist, M. P. Fülscher, and B. O. Roos, Theo. Chim. Acta. **91**, 91 (1995).
[19] M. Rubio, M. Merchán, E. Ortí, and B. O. Roos, Chem. Phys. **179**, 395 (1994).
[20] P. O. Löwdin, J. Mol. Spectrosc. **10**, 12 (1963).
[21] P. Jørgensen, H. J. Aa. Jensen, and J. Olsen, J. Chem. Phys. **89**, 3654 (1988).
[22] J. Olsen, D. L. Yeager, and P. Jørgensen, J. Chem. Phys. **91**, 381 (1989).
[23] J. Rose, T. Shibuya, and V. McKoy, J. Chem. Phys. **58**, 74 (1973).
[24] T. Shibuya, J. Rose, and V. McKoy, J. Chem. Phys. **58**, 500 (1973).
[25] J. Oddershede and P. Jørgensen, J. Chem. Phys. **66**, 1541 (1977).
[26] J. Oddershede, P. Jørgensen, and N. H. F. Beebe, Int. J. Quantum Chem. **12**, 655 (1977).
[27] H. J. Aa. Jensen, P. Jørgensen, H. Ågren, and J. Olsen, J. Chem. Phys. **88**, 3834 (1988).
[28] J. Oddershede, Adv. Quantum Chem. **11**, 275 (1978).
[29] E. K. Dalskov, T. Enevoldsen, H. J. Aa. Jensen, and M. J. Packer, *Technical Notes* (Odense University, 1996).
[30] A. M. Hestenes, *Conjugate Direction Methods in Optimization* (Springer, Berlin, 1980).
[31] J. Olsen, H. J. Aa. Jensen, and P. Jørgensen, J. Comput. Phys. **74**, 265 (1988).
[32] B. O. Roos, M. Fülscher, P.-Å. Malmqvist, M. Merchán, and L. Serrano-Andres, *Quantum Mechanical Electronic Structure Calculations with Chemical Accuracy*, edited by S. R. Langhoff (Kluwer Academic, Netherlands, 1995).
[33] T. Helgaker, P. R. Taylor, K. Ruud, O. Vahtras, and H. Koch, HERMIT, a molecular integral program.
[34] H. J. Aa. Jensen, H. Ågren, and J. Olsen, MOTECC-90 *Modern Techniques in Computational Chemistry*, edited by E. Clementi (ESCOM Science, Leiden, 1990).
[35] A. Hiraya and K. Shobatake, J. Chem. Phys. **94**, 7700 (1991).
[36] P. J. Wilkinson, Can. J. Phys. **34**, 596 (1956).
[37] S. G. Grubb, C. E. Otis, R. L. Whetten, E. R. Grant, and A. C. Albrecht, J. Chem. Phys. **82**, 1135 (1985).
[38] R. L. Whetten, K. J. Fu, and E. R. Grant, J. Chem. Phys. **79**, 2620 (1983).
[39] P. M. Johnson, J. Chem. Phys. **64**, 4143 (1976).
[40] P. M. Johnson and G. M. Korenowski, Chem. Phys. Lett. **97**, 53 (1983).
[41] O. Christiansen, H. Koch, A. Halkier, P. Jørgensen, T. Helgaker, and A. Sanchez de Meras, J. Chem. Phys. (to be published).
[42] J. P. Doering, J. Chem. Phys. **51**, 2866 (1969).
[43] R. H. Huebner, S. R. Mielczarek, and C. E. Kuyait, Chem. Phys. Lett. **16**, 464 (1972).
[44] B. Dick and G. Hohlneicher, Chem. Phys. Lett. **84**, 471 (1981).
[45] D. Bebelaar, Chem. Phys. **3**, 205 (1974).
[46] Y. H. Meyer, R. Astier, and J. M. Leclerq, J. Chem. Phys. **56**, 801 (1972).
[47] H. E. Hunziker, J. Chem. Phys. **56**, 400 (1972).
[48] H. E. Hunziker, Chem. Phys. Lett. **3**, 504 (1969).
[49] M. Allan, J. Electron. Spectrosc. Relat. Phenom. **48**, 219 (1989).
[50] G. A. George and G. C. Morris, J. Mol. Spectrosc. **26**, 67 (1968).
[51] D. E. Mann, J. R. Platt, and H. B. Klevens, J. Chem. Phys. **17**, 481 (1949).